Light scattering spectrum of one-dimensional mixed crystals

J. M. Lopez Castillo and A.-M. S. Tremblay
Département de Physique and Centre de Recherche en Physique du Solide, Université de Sherbrooke, Sherbrooke, Québec, J1K 2R1, Canada
(Received 2 December 1985)

Raman and infrared spectra of linear-chain models of mixed crystals are investigated. Motion along more than one direction is allowed. Much of the phenomenology of real linear-chain compounds such as $ZrS_{3-x}Se_x$ can be qualitatively accounted for: preservation of the Raman and infrared symmetries present in the parent pure compounds, one-, two-, and three-mode behavior, disorder-induced linewidths, and line-shape asymmetries. The physical nature and significance of many of these observed phenomena is clarified.

I. INTRODUCTION

The type of quenched-in disorder present in various condensed systems can sometimes be classified in various categories.[1] Disorder in the positions of the atoms influences the elastic x-ray scattering spectrum for example. This positional disorder coexists with topological order when the disordered lattice can be mapped into an ordered lattice without breaking bonds. Mass and force-constant disorder, on the other hand, have only limited influence on the elastic x-ray spectrum (they enter indirectly in the structure factor), but they manifest themselves drastically in the dynamic properties probed by neutron or light scattering. These spectroscopies are also influenced by the disorder in the effective light-matter coupling constants. The latter disorder (e.g., polarizability for Raman scattering) is clearly not unrelated to the disorder in mass, force constant, or position, but the relation can be quite complicated.

Predicting the detailed light scattering spectrum of a general disordered system, while possible in principle, is an extremely complicated task. Nevertheless, one would like to be able to extract some information on any given disordered system from its light scattering spectrum. Qualitative results can also be extremely useful. For example, it is generally believed that the Raman spectrum of amorphous semiconductors such as[2] Ge or Si reflects the total density of states of these systems because the momentum conservation rule is broken so that more or less all modes become Raman active. While certainly not rigorously valid, this observation may be extremely useful in practice.

Mixed crystals represent a class of systems which in some sense are intermediate between the amorphous solids and the pure crystals. These crystals have only substitutional disorder, i.e., atoms of one kind or another go at random into the sites of an ordered lattice. They thus have relatively little disorder: Their elastic x-ray spectrum looks like that of a pure crystal. They have certainly no topological disorder and the position disorder, if present, is very small. Their light scattering spectrum is also in a certain sense very close to that of the pure systems: take compounds of the type AB_xC_{1-x} for example. The modes observed in the parent compounds (AB or AC) are either both present in the disordered system (two-mode behavior) or a single mode at the average frequency of the parent modes is present (one-mode behavior). Both types of behavior can be explained at least qualitatively by simple *one-dimensional* mass-disorder models.[3,4] In some sense the explanation is based on the Saxon-Hutner-Luttinger theorem[5] which states that for a simple harmonic chain, the disordered system does not have modes in the regions of frequency space where neither parent has eigenmodes. One-mode behavior can (but does not necessarily) occur when the optical bands of the parent compounds overlap. This behavior is confirmed by coherent-potential-approximation calculations,[6] approximate renormalization-group calculations,[7] and simulations.[4,8,9] Note, however, that the accepted nomenclature "one-mode" and "two-mode" behavior is somewhat misleading for reasons which will be discussed in the present paper.

The simplest experimental systems with which one could hope to compare theory and experiment should thus be quasi-one-dimensional. Compounds such as $MS_{3-x}Se_x$ where M is Zr or Hf have been grown and seem to fulfill this requirement.[10,11] Extensive studies of the optical[12–24] and elastic properties[25] of these compounds have appeared. Despite their apparent simplicity, if one includes possible disorder in the mass, coupling constant, first- and second-neighbor force constants, the parameter space needed to describe these compounds is enormous. Detailed fitting of the experimental results would certainly be possible but does not seem especially desirable. The questions we want to answer in this initial study are instead of a qualitative nature. For example, what is the simplest one-dimensional model which exhibits one- and two-mode behavior in its Raman spectrum? (It turns out that some of the qualitative features of the Raman spectrum of AB_xC_{1-x} do not compare well with those of the above real systems.) Why is the Raman line shape in some sense so similar to that of the parent compounds, i.e., are the observed modes narrow because total density of states in the optical bands of the parent compounds are narrow or instead is the positional order helping to preserve the momentum conservation rule which exists in

the pure compounds? How can one explain the apparent preservation of the symmetry classification of the modes even in the disordered compounds? Can the increase of the linewidths with disorder be understood only from the breaking of the wave-vector conservation rule or does one need to invoke a modification of anharmonicities by disorder? What is the relative influence of polarizability (dipole moment) and mass disorder on the light scattering spectrum? Can one extract any information from the line-shape asymmetries (for example, on the curvature of the dispersion relation of the parent compounds)? Clearly, none of the above questions are answered unambiguously by the Saxon-Hutner-Luttinger theorem.[5] Furthermore, this theorem breaks down when one does not consider a strictly one-dimensional model.

Our results should not be interpreted as completely general. In many cases, the part of parameter space which we explored to draw conclusions is relatively small and its choice is guided mainly by physical intuition on the above compounds and not by detailed fitting. Nevertheless, this work lays the ground work for later studies and shows clearly that most of the qualitative features of the optical spectra of the above family of mixed crystals may be understood qualitatively from simple models.

Section II contains preliminaries on Raman and infrared scattering, the method of calculation and the structure of the linear-chain compounds of interest in the present study. Section III contains our results on both a strictly one-dimensional system and on a more realistic model. In Sec. IV we summarize our findings.

II. LIGHT-MATTER COUPLINGS, METHOD OF CALCULATION, AND THE $MS_{3-x}Se_x$ FAMILY

A. Light-matter coupling

We briefly recall a few known facts on Raman and infrared scattering. Since detailed accounts are available in the literature,[26] our discussion is brief and limited to semiclassical images.

In infrared experiments, one usually measures the frequency-dependent reflectivity from which the frequency-dependent dielectric constant is extracted. Through a Kramers-Kronig analysis, one can extract an absorption spectrum which, at a given frequency, is proportional to the square of the component of the oscillating dipole moment which is perpendicular to the line of sight: $\sum_i q_i u_i$ where q_i and u_i are, respectively, the charge and relevant component of the displacement of atom i. To be more specific, let $I(\omega)$ be the intensity of light polarized in the direction x detected at frequency ω, then

$$I^x(\omega)\sim\omega^4\sum_\mu\left[\sum_{i=1}^N q_i\mathbf{u}_i^{(\mu)}\cdot\hat{\mathbf{x}}\right]^2\delta(\omega-\omega_\mu)\ , \tag{2.1}$$

where there is a sum over the N atoms i and, in dimension d, a sum over the dN eigenmodes μ. There are other physical constants and numerical factors coming from geometry, detection efficiency, occupation factors, etc., but they are of no interest in the present study since they only set the overall scale for the detected intensity or, as in the case of the occupation factors, are smooth functions of frequency. In what follows, we always work with $I(\omega^2)$ which is related to Eq. (2.1) by $I(\omega^2)d\omega^2=I(\omega)d\omega$. Hence, we evaluate,

$$I^x(\omega^2)\sim\omega^4\sum_\mu\left[\sum_{i=1}^N q_i\mathbf{u}_i^{(\mu)}\cdot\hat{\mathbf{x}}\right]^2\delta(\omega^2-\omega_\mu^2)\ . \tag{2.2}$$

Note that we do not include Coulomb forces in our calculations. This is justified in ordered crystals[27] when one calculates the frequencies of TO modes extrapolated to the zone center (i.e., through the polariton region). We assume this to be valid also in the disordered systems. All the infrared spectra calculated below are thus for TO modes. We use the terms "transverse" and "longitudinal" to refer to the average direction of oscillation with respect to the chain direction.

Raman scattering, on the other hand, originates from the induced dipole $\vec{\alpha}\cdot\mathbf{E}$, where $\vec{\alpha}$ is the polarizability tensor. When the lattice oscillates at a frequency ω, the polarizability is modulated at the same frequency when $d\vec{\alpha}/dQ\neq0$ (with Q a generalized displacement). Through beating with the electric field, this induces a shift in frequency of the induced polarization. The Raman intensity is proportional to the square of that induced polarization, hence to $(Qd\vec{\alpha}/dQ)^2$. In what follows, we adopt the frequently used model,[28–30] where the total polarizability of the lattice is a sum of the polarizabilities of every chemical bond. Then with $\delta\mathbf{r}_l$ the change in the vector joining the two atoms at the end of bond l, we can write the square of the induced dipole in the direction x when the incident radiation is polarized along z as

$$I^{xz}(\omega^2)\sim(\omega_0\pm\omega)^4\sum_\mu\left[\sum_l\delta\mathbf{r}_l^{(\mu)}\cdot\nabla\alpha_l^{xz}(\mathbf{r})\right]^2\delta(\omega^2-\omega_\mu^2) \tag{2.3}$$

with ω_0 the frequency of the incident radiation. One uses the minus or plus sign depending on whether one is interested in the Stokes or anti-Stokes line.

For the purpose of the following discussion, let us rewrite the sum over bonds in Eq. (2.3) as a sum over lattice sites. We are then left with an expression of the form,

$$I^{xz}(\omega^2)\sim(\omega_0\pm\omega)^4\sum_\mu\left[\sum_{i=1}^N\mathbf{f}_i^{xz}\cdot\mathbf{u}_i^{(\mu)}\right]^2\delta(\omega^2-\omega_\mu^2)\ , \tag{2.4}$$

where $\mathbf{f}_i$ depends on the particular lattice and polarizabilities. Equations (2.2) and (2.4) are functionally very similar and are thus amenable to the unified mathematical treatment described in the following section.

B. Method of calculation

Let us write in matrix notation the equations of motion for the system in the harmonic approximation,

$$(D-M\omega^2)U=0\ , \tag{2.5}$$

where M is a diagonal matrix containing the masses, D is the dynamical matrix, and $U^T=(u_1^x,u_1^y,u_2^x,\ldots,u_N^y)$ in a two-dimensional model, for example. In the classical lim-

it ($\hbar\omega \ll kT$, with T the temperature), both the infrared and Raman intensities (2.2) and (2.4) may be written in the form,

$$I \sim \lim_{\epsilon \to 0} \mathrm{Im} \left[\frac{C}{\omega^2} F^T \frac{1}{D - M(\omega^2 + i\epsilon)} F \right], \tag{2.6}$$

where $C = \omega^4$ for infrared and $(\omega_0 \pm \omega)^4$ for Raman scattering, while $F^T = (f_1^x, f_1^y, f_2^x, \ldots, f_N^y)$ with different values for the f_i depending on whether one is looking at Raman or infrared scattering. To prove Eq. (2.6) note first that it may be rewritten in the form,

$$I \sim \lim_{\epsilon \to 0} \mathrm{Im} \left[\frac{C}{\omega^2} F^T M^{-1/2} \frac{1}{M^{-1/2} D M^{-1/2} - (\omega^2 + i\epsilon)} \times M^{-1/2} F \right]. \tag{2.7}$$

Then, let $V^{(\mu)}$ be the eigenvector for the mode μ,

$$(M^{-1/2} D M^{-1/2}) V^{(\mu)} = \omega_\mu^2 V^{(\mu)} . \tag{2.8}$$

Since the matrix to the left is real and symmetric, it may be diagonalized by an orthonormal transformation made up of the eigenvectors $V^{(\mu)}$. Using this result, Eq. (2.7) may be rewritten in the form,

$$I \sim \sum_\mu \left[\frac{C}{\omega^2} (F^T M^{-1/2} V^{(\mu)}) [(V^T)^{(\mu)} M^{-1/2} F] \times \delta(\omega^2 - \omega_\mu^2) \right]. \tag{2.9}$$

Noting from Eqs. (2.5) and (2.8) that

$$M^{-1/2} V^{(\mu)} = U^{(\mu)} , \tag{2.10}$$

one recovers Eq. (2.4). Note also that the normalization $V^T V = 1$ for every eigenvector means that for any eigenmode,

$$V^T V = U^T M U = \sum_{i=1}^{N} M_i \mathbf{u}_i^2 = 1 , \tag{2.11}$$

which is the correct normalization since the equipartition theorem for harmonic motion leads to a kinetic energy proportional to kT:

$$\frac{\omega^2}{2} \sum_{i=1}^{N} M_i \mathbf{u}_i^2 = \frac{d}{2} kT , \tag{2.12}$$

where d is the dimensionality. This equation explains the factor of ω^2 in the denominator of Eq. (2.6). In the quantum case, one can take the occupation factors into account by the substitution,

$$\frac{kT}{\omega^2} \to \frac{\hbar}{\pm\omega} \left[\frac{1}{e^{\pm\hbar\omega/kT} - 1} \right] \tag{2.13}$$

with the minus sign for the Stokes intensity and the plus sign for the anti-Stokes intensity.

In what follows, the "projected density of states," Eq. (2.6) is evaluated by transfer matrix methods which are generalizations of the negative-eigenvalue theorem which is often used to compute total densities of states.[31] The method has been described briefly in Ref. 8 and in more details in Ref. 32. We can summarize the idea as follows. One first notes that Eq. (2.6) may be obtained from the second derivative with respect to Θ of the following generating function:

$$\mathcal{F} = \ln \left[\int \mathcal{D}Z \exp[-\tfrac{1}{2} Z^T (D - M(\omega^2 + i\epsilon)) Z + \Theta F^T Z] \right], \tag{2.14}$$

where $Z^T = (z_1^x, z_1^y, \ldots, z_N^y)$, and

$$\int \mathcal{D}Z = \prod_{i=1}^{N} \int_{-\infty}^{\infty} dz_i . \tag{2.15}$$

The matrix D is then written in block tridiagonal form in such a way that the problem becomes strictly one dimensional for the blocks containing information on the degrees of freedom in every "unit cell." One then generates recursion formulas for the generating function and its relevant derivatives by evaluating the Gaussian integrals one unit cell at a time. This method can be seen as a way to optimize Gaussian elimination for the sparse matrices of interest here.

Finally, we should note that in practice the calculations are naturally performed with finite values of ϵ. The δ functions in Eq. (2.4) are then replaced by Lorentzian functions. This is a very convenient way of introducing phenomenologically the natural linewidth which is due to anharmonicities. We chose a value of ϵ which leads to the correct order of magnitude for the linewidths of the pure compounds. Note that the larger ϵ the smaller the system size needed to achieve convergence. This is easy to understand intuitively because in the presence of large damping the modes can propagate only over short distances. In the numerical results presented below, we used system sizes large enough to insure convergence.

C. The $MS_{3-x}Se_x$ family of compounds

The crystallographic structure of these compounds, illustrated in Fig. 1, has been described in detail in Refs. 10

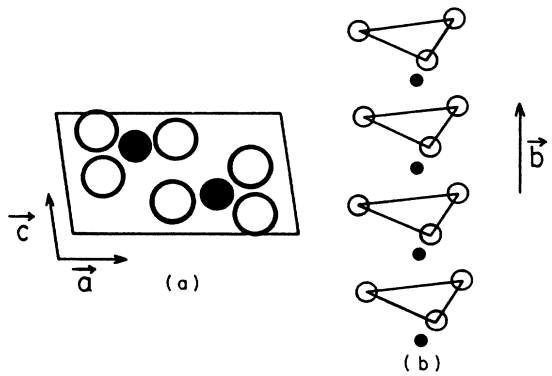

FIG. 1. Structure of $ZrS_{3-x}Se_x$-type compound. (a) Projection in the xz plane of a unit cell. Open circles are S or Se atoms and solid circles are Zr atoms. The Zr atoms of one chain are at the same distance along the b axis as the chalcogens of its neighboring chain. (b) Structure along one chain direction (from Ref. 34).

and 11. Roughly speaking, they are made up of weakly coupled pairs of chains. There are eight atoms per unit cell. Each chain in a pair is weakly coupled through van der Waals forces to its companion. A chain is made up of a perfectly ordered sublattice of M atoms (either Zr or Hf). In between every pair of M atoms, there are chalcogen atoms (S or Se) on an isosceles triangle whose plane is perpendicular to the chain axis. In the mixed crystals, S and Se can occupy any chalcogen site and the positions of the atoms do not differ from those of the corresponding pure compounds by much: x rays[33,34] reveal a small change in average lattice constants.

In what follows, we consider a single chain and assume that it is completely independent of other chains. Nevertheless, we should note that in the real compound, the fact that there are two chains per unit cell leads to pairs of modes very close in frequency, one of which is infrared active while the other is Raman active. This comes from the fact that an infrared mode of a single chain can be either active or inactive in infrared spectroscopy depending on whether its companion chain is oscillating in or out of phase. In the latter case, there would be some Raman activity coming, in a bond-polarizability model, from the interchain bonds. The fact that in the real compound such Raman-infrared pairs of modes are close in frequency reflects the fact that the chains are weakly coupled. Clearly, our calculations of intensities and line shapes have a chance of being realistic mainly when we model modes that are seen in the same spectroscopy (either Raman or infrared) in both the single- and double-chain system.

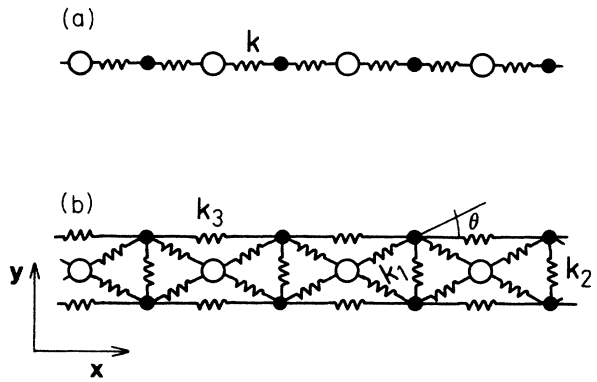

FIG. 2. (a) One-dimensional chain AB_xC_{1-x}. A atoms are located regularly on the open circles sublattice. B and C atoms are independently distributed on the solid circle sublattice with respective probabilities x and $1-x$. There is no force-constant (k) disorder. Motion in only one direction is allowed. (b) "Three-atoms-per-unit cell" model AB_xC_{2-x}. A atoms occur regularly on the open circles. The "chalcogen" atoms B and C are independently distributed on the solid circles with respective probabilities $x/2$ and $(2-x)/2$. There is no force-constant disorder but the metal-chalcogen force constant k_1, nearest-neighbor, k_2, and next-nearest-neighbor, k_3, chalcogen-chalcogen force constants differ. The latter force constant is necessary for stability. The diagonal bonds k_1 form a $\pi/6$ angle with the horizontal axis. Motion is allowed in the plane.

III. MODELS AND RESULTS

A. Strictly one-dimensional chain

The simplest model representing substitutional disorder in mixed crystals of the type $MS_{3-x}Se_x$ is that of a linear harmonic chain AB_xC_{1-x} in which atoms A of mass M_A are on a periodic sublattice while atoms B and C with masses M_B and M_C are placed independently on the sites of the other sublattice with probabilities x and $1-x$, respectively [see Fig. 2(a)]. This model is clearly inadequate in general, but should have some of the qualitative features of modes of the real chain when they involve motion of the M atoms and of the chalcogen cages as a whole.

1. Infrared spectrum

The infrared spectrum of the strictly one-dimensional chain has been extensively studied before[4,8,9] and this section only summarizes some of the main results.

Motion along only one direction is considered. The infrared absorption spectrum is approximated by what can be interpreted as the density of states projected on the zone-center optical branch. More specifically, referring to Eq. (2.2), we have

$$I(\omega^2)\sim\omega^4\sum_{\mu}\left[\sum_{i=1}^{N}q_i u_i^{(\mu)}\right]^2\delta(\omega^2-\omega_\mu^2)\ . \tag{3.1}$$

The factor in front of the δ function can be interpreted as the square of the projection of the displacement vector $U=(u_1,u_2,\ldots,u_N)$ on the vector $\phi^T=(Q_1,Q_2,\ldots,Q_N)$ which, when $Q_i=(-1)^i$, has the same symmetry as the vector describing the amplitude of a plane wave in the zone-center optic mode of the linear binary chain.

Previous investigations[4,8,9] have shown that one sees one or two optically active bands in the mixed crystals with mass disorder only. Such behavior is often referred to as one- or two-mode behavior, but we wish to stress here that, in general, one gets contributions to the infrared intensities from a wide range of frequencies covering a large portion of the optical bandwidth of the parent compounds so we shall use the terminology[6] one-band and two-band behavior.

To be more specific, let us describe one- and two-band behavior in more details as observed[8,9] in the one-dimensional model with mass disorder only. In the case where the optic bands of the parent compounds AB and AC do not overlap, only two-band behavior can be observed.[3,5] The modes closest to the original two zone-center optic modes are more intense but, in general, a large fraction of the modes in the energy range corresponding to the optic bands of the parent compounds are excited. The modes at or very close to the optic band edges of the pure compounds do not usually contribute appreciably. The relative weight of the two bands depends on the concentration.

When the optic bands of the parent compounds overlap, the infrared activity is in the frequency interval $\Delta\omega^2$ between the two zone-center optic modes of the parent compounds. Sometimes, one can see that the active frequencies shift slowly with concentration from the infrared ac-

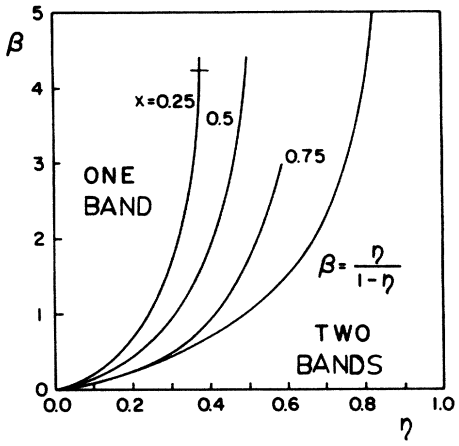

FIG. 3. Mass parameters for one-band and two-band behavior in the strictly one-dimensional AB_xC_{1-x} model with mass disorder (from Ref. 8). $\beta=M_B/M_A$ and $\eta=1-M_C/M_B$ ($M_C<M_B$). Other methods of calculation (e.g., Ref. 6) give qualitatively similar results.

tive mode of one of the parent compounds to that of the other. The width of the excited band is, in general, a sizable fraction of $\Delta\omega^2$. Very often, at a given concentration, one sees a crossover to two-band behavior, i.e., there are two excited bands with a clear gap in between. Around the crossover, most of the interval $\Delta\omega^2$ is infrared active.

For the sake of completeness, we have reproduced in Fig. 3 the diagram showing the regions of parameter space in the mass-disorder model where the various types of behavior are observed. Note that one-band behavior is, in general, observed for small values of $1-M_C/M_B$ where $M_C<M_B$, in other words when the perturbation due to mass disorder is relatively small and the infrared active modes of the parent compounds are close. The atom A which repeats must also not be too heavy, otherwise atoms B and C hardly influence each other. We also want to stress that in either one- or two-band behavior, a whole range of eigenfrequencies of the disordered system become active. Within the present model, the natural linewidth of the individual eigenfrequencies (modeled here by ϵ) is the same in the disordered and ordered cases. It is only when the natural linewidths of the excited eigenfrequencies overlap that the infrared spectrum looks as if only one or two modes were excited. We exhibit explicit examples of this in the discussion of the more elaborate model in Sec. III B.

2. *Raman spectrum*

Following Eq. (2.3), in a model where the total polarizability is a sum of bond polarizabilities, the Raman spectrum of the one-dimensional chain is proportional to

$$I(\omega^2)\sim\sum_{\mu}\left[\sum_{l}a_l(u_{1l}^{(\mu)}-u_{2l}^{(\mu)})\right]^2\delta(\omega^2-\omega_\mu^2)\,, \qquad (3.2)$$

where a_l is related to the derivative with respect to length of the polarizability of the bond l and u_{1l} and u_{2l} are the displacements of the atoms at either ends of the bond. Let us rewrite Eq. (3.2) as a sum over site instead of bonds. We find

$$I(\omega^2)\sim\sum_{\mu}\left[\sum_{i}(a_{i,i+1}-a_{i,i-1})u_i^{(\mu)}\right]^2\delta(\omega^2-\omega_\mu^2)\,, \qquad (3.3)$$

where $a_{i,i+1}$ and $a_{i,i-1}$ are the polarizability derivatives for the bonds between atom i and its two neighbors.

Systems which possess an inversion center cannot be Raman active if they are infrared active and vice versa. Nevertheless, this selection rule does not necessarily apply to disordered systems so it is legitimate to ask what is the Raman spectrum of the mixed chain. We consider two cases. First, suppose that there is no polarizability disorder, i.e., the polarizabilities of the two types of bonds (AB or AC) are the same. Then it is clear that the sum within large parentheses in Eq. (3.2) reduces to zero. There is no Raman active mode.

Second, assume that the polarizabilities of bonds AB and AC differ. Equation (3.3) shows that this time, the displacement vector is projected on a vector proportional to $\phi^T=(\epsilon_1,0,\epsilon_3,0,\ldots,\epsilon_N)$ where the ϵ_i are independent random variables which can take the value $-1,0,1$ and whose average is zero. Note that B- and C-type atoms in this case are surrounded by identical bonds and hence are projected on a 0 in the vector ϕ. Typical spectra obtained in this case are shown in Fig. 4. The factor ω^{-2} coming from the normalization [Eq. (2.12)] has been omitted in this figure. This avoids having to plot the ω^{-2} divergence at low frequencies. The following qualitative remarks are of interest: The spectrum is very different from the corresponding infrared spectrum and also from the total density of states. Nevertheless, where the intensity is strong there is also a corresponding large density of states and the modes involve mainly motion of the atoms A on the ordered sublattice. The latter result is expected when one considers the explicit expression for the vector ϕ. The rough shape does not depend too much on concentration and the Saxon-Hutner-Luttinger theorem[5] is clearly satisfied since active modes are within the bands of the parent compounds.

We digress in passing to note that in the mixed crystal there is one finite-frequency eigenstate which is extended,

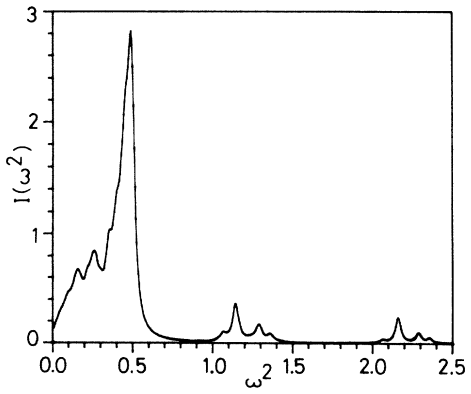

FIG. 4. Raman spectrum, in arbitrary units, for the strictly one-dimensional model. $M_A=4$, $M_B=2$, $M_C=1$, $\epsilon=0.01$, $k=1$, $x=\frac{1}{2}$. Chain length, 2000 atoms. A factor ω^{-2} has not been included in the spectrum.

namely the band-edge mode where only the ordered sublattice is moving. In that mode, the B and C ions are not moving hence their mass is irrelevant and the disorder does not show up, which means a truly extended eigenstate. We note that the strongest Raman intensity in the figures happens to lie near this extended state but that mode itself is not Raman active. This can be seen by noting that magnitude of the displacements of the A atoms are all identical in this mode, which means that its intensity is

$$I \sim \frac{1}{N}\left[\sum_i (-1)^i \epsilon_i\right]^2, \tag{3.4}$$

where the factor $1/N$ comes from the normalization for an extended state. Since the ϵ_i are random variables with zero average, the average of the square of the sum in Eq. (3.4) is of order N, which means that the intensity is independent of N, instead of growing linearly with N and hence is negligible. The large Raman intensity near this mode is thus largely due instead to the large density of states in this region.

B. The model with three atoms per unit cell

Careful experimental investigations[20,21,34] have demonstrated the importance of the S_2 or Se_2 molecule in the pure chains to explain the spectrum of the $MS_{3-x}Se_x$ compounds. It is the absence of these molecular modes and the absence of motion in a perpendicular direction which are the main defects of the strictly linear-chain model. The simplest model which includes the "molecular" modes is illustrated on Fig. 2(b). The atoms are allowed to move in the plane, which means that there are six degrees of freedom per unit cell in this model instead of two as in the preceding one. The forces between the atoms are central, hence rotationally invariant.[35] The parameter space is potentially enormous but we restrict ourselves to three masses (M_A, M_B, M_C), two nearest-neighbor force constants (k_1, k_2), one second-neighbor force constant (k_3), two polarizabilities (metal-chalcogen and chalcogen-chalcogen bond), and one angle θ. Note that we have only mass disorder. The parameter θ is clearly irrelevant as long as it is within a reasonable range (we take $\theta = \pi/6$), so that given the arbitrariness in the choice of units for mass, frequency, and scattering intensity, we are left only with two mass ratios, two force-constant ratios, and one polarizability ratio as parameters. The behaviors we discuss below are "generic" in the sense that they can occur for sizable ranges of parameters.

The zone-center and zone-edge modes of the pure compounds are schematically represented in Table I along with the formula for their eigenfrequencies. Figure 5 is a schematic representation of the dispersion curves for the pure compounds. Note that for all wave vectors K, the

TABLE I. Eigenmodes of the pure chain near the zone center and zone edge for the model of Fig. 2(b). M stands for the A atom on the periodic sublattice, while m stands for B or C. The definitions of the force constants k_1 to k_3 and of the angle θ are given in Fig. 2(b). A is for acoustic, R for Raman, IR for infrared. L (longitudinal) and T (transverse) refer to the direction of motion with respect to the chain direction. T and L in the usual notation LO and TO for infrared modes have a different meaning: we are always computing TO frequencies. The first two columns of the last four rows are the optical modes which are discussed in this work.

	Zone center		Zone edge	
Name	Symmetry	ω^2	Symmetry	ω^2
Longitudinal acoustic (LA)	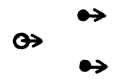	0	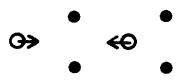	$4\frac{k_1}{M}\cos^2\theta$
Transverse acoustic (TA)		0		$4\frac{k_1}{M}\sin^2\theta$
Longitudinal infrared (LIR)	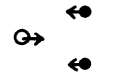	$2\frac{k_1}{m}\cos^2\theta\left[1+\frac{2m}{M}\right]$	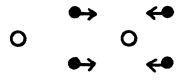	$\frac{2}{m}(k_1\cos^2\theta+2k_3)$
Transverse infrared (TIR)		$2\frac{k_1}{m}\sin^2\theta\left[1+\frac{2m}{M}\right]$	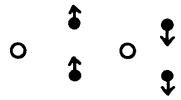	$\frac{2}{m}k_1\sin^2\theta$
Longitudinal Raman (LR)	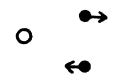	$\frac{2}{m}k_1\cos^2\theta$	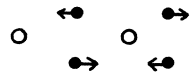	$\frac{2}{m}(k_1\cos^2\theta+2k_3)$
Transverse Raman (TR)	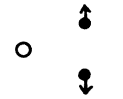	$\frac{2}{m}(k_1\sin^2\theta+k_2)$	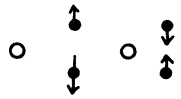	$\frac{2}{m}(k_1\sin^2\theta+k_2)$

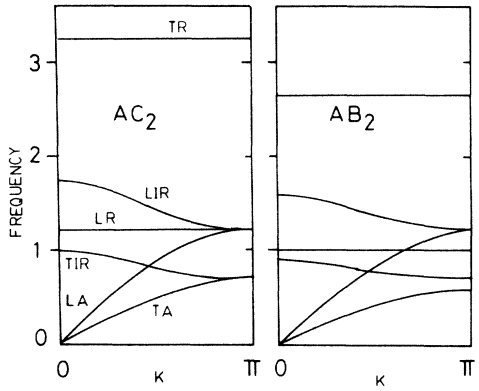

FIG. 5. Sketch of the dispersion relations $\omega(K)$ for the model of Fig. 2(b) at the extremal compositions. ω is the frequency and K the wave vector. $M_A=2$, $M_B=1.5$, $M_C=1$, $k_1=1$, $k_2=5$, $k_3=0$. The notation for the branches is defined in the table. Note that the Raman branches LR and TR are flat. The former has some curvature, however, when $k_3\neq 0$. The TR branch is at sizably larger frequencies than the other modes because of the large value of k_2. This corresponds to the strong chalcogen-chalcogen force constant inferred experimentally.

eigenmodes involve motion either purely along the chain or purely transverse to it. We also stress once more that longitudinal and transverse in the case of the infrared modes refers here only to the direction of the displacements of the atoms relative to the chain direction. The infrared frequencies that we are calculating are those of the TO (transverse) modes in the usual notation.[27] [See discussion below Eq. (2.2)].

Since there is no polarizability or charge disorder in our model, the components of the vectors ϕ on which the eigenstates must be projected to compute the light scattering intensities are the same in every unit cell, which can also be stated as meaning that the density of states is projected at $K=0$. Hence, we only need to specify the six components of ϕ in a unit cell. Let the chain axis be along the x axis. Then let the first two components correspond, respectively, to the x and y displacement of the M atoms, the third and fourth to the x and y displacements of the top chalcogen atom, and the fifth and sixth to the displacements of the other chalcogen.

The vector,

$$\phi_1^T=(2,0,-1,0,-1,0) \tag{3.5}$$

gives the infrared intensity of the dipole along the chain direction, while

$$\phi_2^T=(0,2,0,-1,0,-1) \tag{3.6}$$

gives the intensity in the perpendicular direction.

For the Raman intensity, suppose that for a given bond in the $\mathbf{r}$ direction, the polarizability tensor is given by[28–30]

$$\vec{\alpha}=\alpha(|r|)\hat{r}\hat{r} \tag{3.7}$$

with $\hat{r}$ a unit vector. Then,

$$\delta\mathbf{r}\cdot\nabla\alpha_{pq}=\left[\frac{\partial\alpha}{\partial r}-\frac{\alpha}{r}\right]\hat{r}_p\hat{r}_q(\hat{r}\cdot\delta\mathbf{r})+\frac{\alpha}{r}(\delta r_p\hat{r}_q+\hat{r}_p\delta r_q)\ , \tag{3.8}$$

where δr_p is the p component of the difference between the displacement vectors of the atoms spanning the bond. Explicit evaluation and gathering of all the factors multiplying a given atomic displacement leads, within numerical factors, to

$$\phi_3^T=(0,0,1,0,-1,0) \tag{3.9}$$

for I^{xy} and

$$\phi_4^T=(0,0,0,1,0,-1) \tag{3.10}$$

for I^{xx}. Note that since the polarizability tensor is symmetric for every bond, $I^{xy}=I^{yx}$ for the system as a whole. Furthermore, while I^{xx} is not the same as I^{yy}, they are proportional, hence Eqs. (3.9) and (3.10) suffice to compute the Raman active modes.

Note that the symmetries of the vectors [Eqs. (3.5) and (3.6) and (3.9) and (3.10)] correspond to those of the zone-center optic modes of the pure compounds illustrated in Table I. Note also that if we add the two vectors,

$$\phi_5^T=(1,0,1,0,1,0)\ , \tag{3.11}$$

$$\phi_6^T=(0,1,0,1,0,1)\ , \tag{3.12}$$

corresponding to the two acoustic branches, the set ϕ_1 to ϕ_6 forms an orthogonal basis for the $K=0$ projections of the density of states.

1. *Infrared spectrum*

In all the spectra illustrated in this section, the factor of ω^4 appearing in Eq. (2.2) has been dropped. This is a smooth factor that does not change the sharp features of the spectra.

We consider in turn the longitudinal and transverse modes. Figure 6 illustrates the evolution of the spectrum for the longitudinal mode as a function of composition.

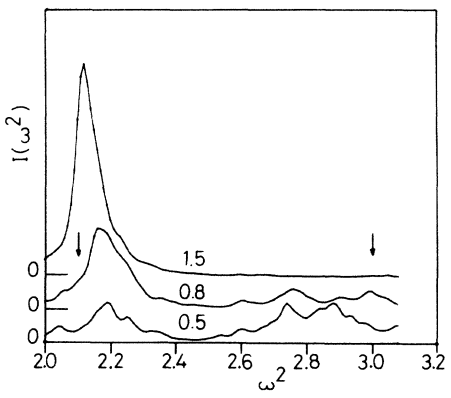

FIG. 6. Evolution of the longitudinal infrared mode as a function of composition x for the model AB_xC_{2-x} of Fig. 2(b). $\phi^T=(2,0,-1,0,-1,0)$, $M_A=2$, $M_B=2.5$, $M_C=1$, $k_1=1$, $k_2=5$, $k_3=1.5$, $\epsilon=0.01$. Chain length, 115 cells (345 atoms). The vertical scale is arbitrary.

The compound is AB_xC_{2-x} and x takes the values 1.5, 0.8, and 0.5. The masses are chosen such that the ratios $2M_B/M_A$ and $2M_C/M_A$ are approximately equal to the corresponding ratios of total chalcogen (3Se for $2B$ or 3S for $2C$) mass to zirconium mass in the $ZrS_{3-x}Se_x$ compound. The chalcogen-chalcogen force constant is relatively large because the molecular modes most influenced by that force constant are at relatively high frequencies as will become apparent below when we discuss the Raman spectrum. Figure 6 shows that, in general, one expects a large fraction of the band between the optic mode frequencies of the corresponding pure compounds (marked by arrows) to be excited. The width ϵ of the individual Lorentzian peaks forming the spectrum has been chosen to fit roughly the observed widths in the pure compounds. If anharmonicities are larger in the disordered compound, the spectra would be smoothed out even more and Fig. 6 might well then be interpreted as a change from one-band to two-band behavior around $x=0.5$. On the other hand, within the resolution of Fig. 6, a few peaks could be taken literally as "modes" in the experiments. In fact, there are often such stray peaks appearing in the experimental spectra for midrange compositions. They are often interpreted as "impurity modes" but the extra modes we see here are not associated with any kind of extrinsic impurities.

The purely one-dimensional chain of Sec. III A has infrared spectra which are qualitatively similar to those of Fig. 6. Since it is known[4,8,9] that this one-dimensional chain can exhibit one-band behavior, it is legitimate to ask whether this behavior persists for the more complicated model and whether the mechanism in the latter case is similar to that invoked in the former case. Figure 7 displays a spectrum where only one band is observed. Figure 8 illustrates the evolution of the peak frequency with composition. This is clearly what one would call one-band behavior. The heights of the vertical bars are about equal to the observed widths of the mode. Note from Fig. 7 that as mentioned for the strictly one-dimensional chain, the width of the mode in the strongly

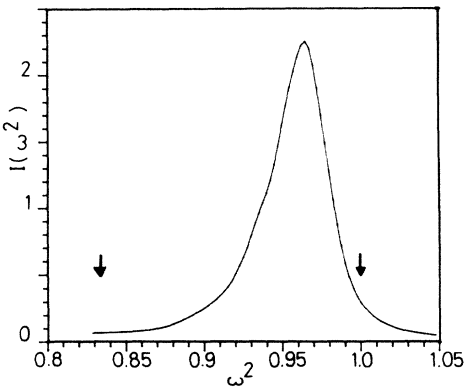

FIG. 7. One-band behavior for the transverse infrared mode of the model AB_xC_{2-x} of Fig. 2(b) at composition $x=0.5$. $\phi^T=(0,2,0,-1,0,-1)$, $M_A=2$, $M_B=1.5$, $M_C=1$, $k_1=1$, $k_2=5$, $k_3=0$, $\epsilon=0.01$. Chain length, 500 cells (1500 atoms). Vertical scale arbitrary. Note that the natural linewidth $\delta\omega^2\approx 2\epsilon$ is an appreciable fraction of the frequency interval between the optic modes of the pure compounds.

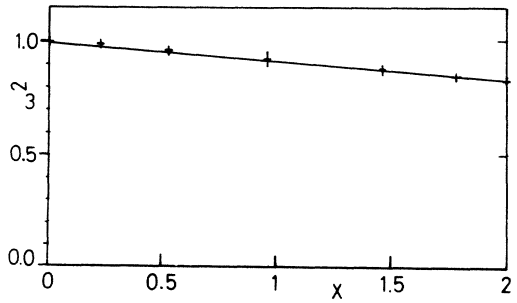

FIG. 8. One-band behavior in an infrared mode: Evolution of the peak frequency as a function of composition for the parameters of Fig. 7. Height of the vertical bars is about equal to the bandwidth. The plot appears linear whether frequency or frequency square is used in ordinate. The compositions studied are $x=0$, 0.2, 0.5, 1.0, 1.5, 1.8, 2.0.

disordered regime, here $x=0.5$, is a sizable fraction, about $\frac{1}{4}$, of the frequency interval between the infrared active modes (indicated by arrows) of the pure compound. The real system $ZrS_{3-x}Se_x$ has a comparable ratio of linewidth to frequency difference between extremal compositions.[19] Clearly, that width comes from the fact that many eigenmodes are infrared active in the disordered compound. It is not induced by anharmonicities. With the value of ϵ chosen here, these could account for only half of the linewidth. Contrary to the strictly one-dimensional chain, the line shape here can be modified by changing the force constants to move other optic branches closer or farther away from the region of interest. Finally, note that the masses were chosen so as to be in the one-band region of Fig. 3. This was done so as to make the infrared modes of the pure compounds as close in frequency as they are in the real system. In the latter case though, this occurs because the force constants in the ZrS_3 and $ZrSe_3$ compounds differ contrarily to the present model.

2. *Raman spectrum*

Of the two Raman branches, the tranverse Raman (TR) branch, which involves molecular motion of the "chalcogen," (B and C atoms), is most closely related to experiment. The longitudinal Raman (LR) mode, on the other hand, is not a molecular mode in the sense that in the presence of disorder, the A atoms are strongly involved in all eigenstates. This LR mode also has no even approximate analog in the strictly one-dimensional chain. Its spectrum in the parallel-perpendicular configuration I^{xy} is exhibited in Fig. 9. Most of the band between the pure compound modes is activated, but the structure is complex and differs from a simple density of states. That type of behavior is often observed in our spectra. Note also that when higher-frequency modes of the pure compounds are close to the frequency range of interest, they are activated as well.

Let us come back to the more interesting transverse Raman mode. A glance at Table I and at Fig. 2(b) immediately suggests that with a strong chalcogen-chalcogen bond, we are dealing with molecularlike modes. Figure 10

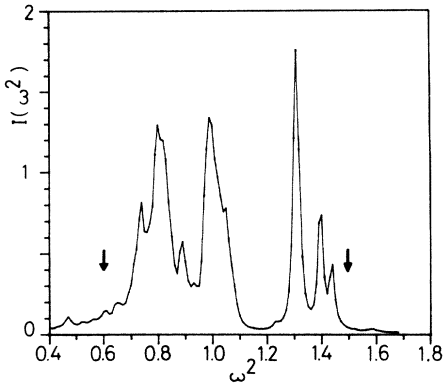

FIG. 9. Longitudinal Raman spectrum, in arbitrary units, for the model AB_xC_{2-x} in the parallel-perpendicular configuration I^{xy} for $x=1$. $\phi^T=(0,0,1,0,-1,0)$, $M_A=2$, $M_B=2.5$, $M_C=1$, $k_1=1$, $k_2=5$, $k_3=-0.35$, $\epsilon=0.01$. Chain length, 500 cells (1500 atoms). Note that the activated frequency range is between the two Raman frequencies of the pure chains. Some activation persists outside that range but is quite small.

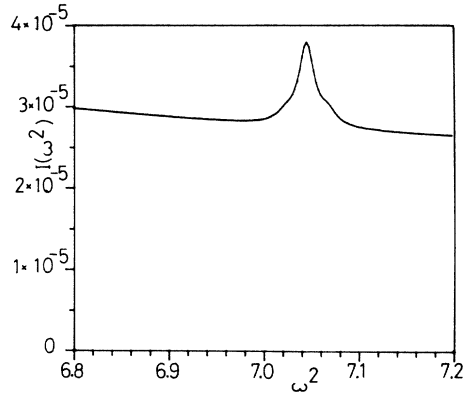

FIG. 11. The TR left-hand (B-B≈Se-Se) mode of Fig. 10 seen in transverse infrared configuration, $\phi^T=(0,2,0,-1,0,-1)$. The height of infrared active modes on that scale is comparable to that of Raman active modes in Fig. 10. The background intensity comes from the tails of the Lorentzians of the transverse low-frequency infrared modes.

illustrates the spectrum in the parallel-parallel I^{yy} configuration for $x=1$. This is clearly a so-called three-mode behavior, very analogous to that observed in $MS_{3-x}Se_x$, where M is[21,22,34] Zr or[20] Hf. The left- and right-hand peaks are associated, respectively, with Se-Se and S-S vibrations while the center peak comes from the S-Se "molecules." All frequencies are slightly higher than one would expect from the isolated molecules. Two factors contribute to the sharpness of the lines: First, the bands of the original compound are flat, which means that the molecules there are vibrating independently of one another; and second, the frequencies are much higher than any of the other ones of this compound, leading, from a simple perturbative point of view, to modes that are not influenced by any other because of large energy denominators.

Most importantly, this TR spectrum allows us to exhibit two important general facts. First, and in a sense as expected, the Saxon-Hutner-Luttinger[5] theorem is not satisfied for this model, i.e., the S-Se mode appears in a frequency range where both of the parent compounds had a gap. This nonapplicability of the theorem is apparent in other spectra we have calculated but here it is most obvious. Second, the categories Raman, infrared, longitudinal, and transverse for this model remain a good classification even in the disordered compounds. This is demonstrated by Figs. 11 and 12. Figure 11 shows the transverse infrared (TIR) spectrum in the frequency range of the left-hand Se-Se peak of Fig. 10. Even though there is a small peak at the expected frequency, the intensity is a factor 10^5 smaller than that of the other infrared active modes hence completely negligible. For a pure chain of the same length we did not see that peak, which indicates that the small intensity observed in the disordered compound is not an end effect but instead is due to the breakdown of the infrared-Raman exclusion rule of the pure compounds. For all practical purposes though, one can consider this exclusion rule as still valid. The intensity at

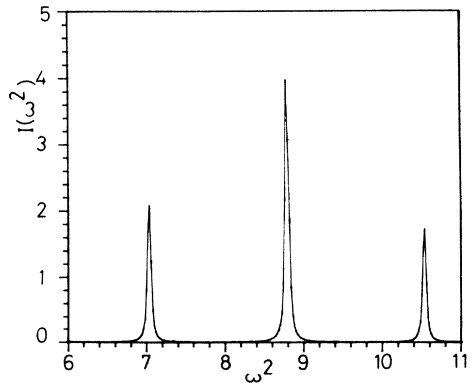

FIG. 10. Transverse Raman spectrum, in arbitrary units, for the model AB_xC_{2-x} in the parallel-parallel configuration I^{yy} for $x=1$. $\phi^T=(0,0,0,1,0,-1)$, $M_A=2$, $M_B=1.5$, $M_C=1$, $k_1=1$, $k_2=5$, $k_3=0$, $\epsilon=0.02$. Chain length 500 cells (1500 atoms). B-B and C-C vibration frequencies, respectively, $\omega^2=7$ and $\omega^2=10.5$.

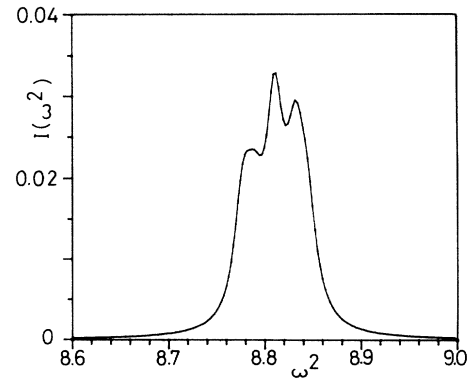

FIG. 12. The TR intermediate (B-C≈S-Se) mode of Fig. 10 seen in transverse infrared configuration, $\phi^T=(0,2,0,-1,0,-1)$. The height of infrared active modes on that scale is comparable to that of Raman active modes in Fig. 10.

that frequency in the I^{xy} Raman configuration and longitudinal infrared (LIR) configurations were even smaller than that in Fig. 11. For the middle peak of Fig. 10, on the other hand, which arises purely from the disorder, one might expect that the symmetries just discussed are more strongly broken. The fact that this is indeed the case is shown by Fig. 12, which represents the transverse infrared spectrum in the S-Se frequency range. In this worse case (the intensity was even smaller, 10^{-4} to 10^{-5}, in the other configurations) the intensity is roughly a factor of 100 smaller than that of the infrared active modes, so even though the exclusion is not as good as for the Se-Se peak, for all practical purposes the symmetry classification of the pure compounds is still valid. It should also be clear that the exclusion transverse-longitudinal is stronger than the exclusion Raman-infrared since in all cases, the TR modes had an intensity in the TIR configuration stronger than in the LR one.

3. *Line-shape asymmetries and correlated disorder*

Attention of various groups has been focused recently on line-shape asymmetries.[36–40] In all cases, the mechanism proposed for asymmetric line shapes is similar: In the mixed, or disordered, crystal the momentum conservation rule is broken, so it is assumed that the modes near the optically active modes of the pure compound will also be excited. This means, for example, that for an optic branch whose highest frequency is an active zone-center mode, disorder will induce a broadening of the line on the low-frequency side.

The above mechanism is easily checked for the strictly one-dimensional model.[41] Suppose that in a "two-band" case, one looks at the infrared spectrum near the highest-frequency mode of the AC compound. For small concentrations of B, one observes a broadening of the line towards the lower frequencies. With small enough ϵ, one can resolve individual peaks which can in turn be put in correspondence with the highest possible frequency of small segments of the AC chain. Noting that the infrared mode of short segments of AC compounds are all smaller than that of the infinite compound, the asymmetry towards low frequencies is immediately explained. The intensity of a peak is then proportional to the probability of obtaining a segment of the necessary length, so in this case it is clear that correlations between the occupation of different sites will reduce the line-shape asymmetry since longer segments of the AC compound will become more probable.

Line-shape asymmetries are also observed in the $MS_{3-x}Se_x$ type of materials.[20,21,42] Since these compounds are too small to be analyzed by neutron scattering, experimental information on the dispersion relations of the zone center is not available. It would thus be valuable if, as suggested by the above discussion, one could associate the line-shape asymmetries of the optical spectra with curvature of the bands of the pure compounds.

The top curve in Fig. 13 is a magnified view of the line shape of the B-B (Se-Se) vibration observed in Fig. 10. Each chalcogen lattice position in this case is occupied with independent probabilities. This line is clearly asymmetrical. Since the optical branch of the pure compound is in this case flat, the direction of the asymmetry here is in no way related to the dispersion relation. One should thus be aware that the explanation of line-shape asymmetries in terms of band curvature is not universally applicable.

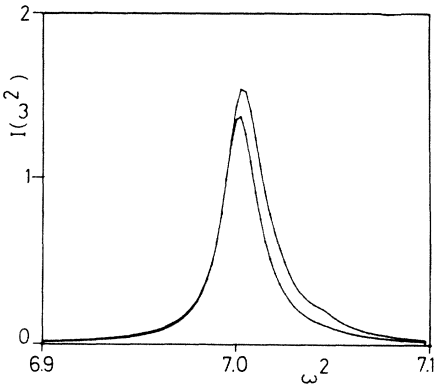

FIG. 13. Line shape of the TR left-hand (B-B≈Se-Se) mode of Fig. 10 as a function of correlations. No correlations for the upper curve, and perfect intracell correlations for the lower curve. The intensity is normalized differently for the two curves to illustrate the fact that the left-hand side of both lines have identical shapes. $x=1.8$, $\epsilon=0.01$. Chain length, 1000 cells (3000 atoms). Note that in the case of no correlations, the bump on the high-frequency side develops into a peak for smaller values of x.

The line-shape asymmetry is nevertheless also reduced when correlations are added to the model. We have studied various intermediate cases but it is perhaps more instructive to look at the limiting case where there is perfect correlation within a unit cell and no correlations between cells. In other words, the occupation of different unit cells is independent, but a given cell can only be occupied by two chalcogens of the same kind. The spectrum then obtained is the lower curve in Fig. 13. Clearly, the disorder-induced asymmetry has disappeared. In fact, the line basically has its zero disorder width 2ϵ because the oscillations in each cell are now independent given that the k_3 bonds are central forces. Note that we have reduced the vertical scale in the perfect correlation case to show that the low-frequency side of the line is the same with or without correlations.

Finally, note that the asymmetry observed for the C-C (S-S) line is very similar to that of the B-B (Se-Se) line in Fig. 13. While this asymmetry is towards higher frequencies for both of these lines, in the real compound the S-S line shape extends towards the lower frequencies, although in this case the asymmetry is less pronounced than for the Se-Se line.

IV. CONCLUSIONS

While the purely linear-chain model has been used for a number of years[4] as a model to understand optical properties of mixed crystals, it is only recently that it has been possible to do experiments on real linear-chain compounds.[12–23] This is particularly important because it is only on these one-dimensional systems that all the

features of the linear-chain model can possibly be realistic. Indeed, it is known[4] that some properties of the linear-chain model are qualitatively different from the corresponding properties of higher-dimensional systems. For example, it is known that all states are localized in one dimension while a mobility edge exists in higher dimensions.[43] Hence the linear-chain model can be compared to results on higher-dimensional systems only with extreme caution.

Unfortunately, the simplest linear-chain compounds[10–23] $M\mathrm{S}_{3-x}\mathrm{Se}_x$ do not quite have the structure of the linear-chain model: Motion is allowed in more than one direction and the unit cell is more complicated, yielding "molecularlike" modes. We have thus studied the simplest model which in our opinion has all the qualitative features of the real compounds. The model is exhibited in Fig. 2(b). We considered mainly the effect of mass disorder. We recall that our purpose was not detailed fitting. Such a task is arduous enough for the pure compounds,[24] in this first analysis it would only mask the physics of the results. What has been accomplished is summarized in the following paragraphs: (1) to (4) discuss results that are specific to our model and cannot be inferred from the strictly linear chain, while the results mentioned in the following paragraphs are equally valid in the strictly one-dimensional chain and in our model.

(1) The best-established result for the purely one-dimensional chain with one degree of freedom per atom is the Saxon-Hutner-Luttinger theorem.[5] Perhaps the most obvious feature [cf. the frequency of the S-Se molecular mode (Fig. 10)] of our results is that this theorem does not apply for our model. Hence, while the $M\mathrm{S}_{3-x}\mathrm{Se}_x$ family could have been thought of as a good realization of the linear-chain model, some of its features are qualitatively different from those of the linear chain.

(2) Our model reproduces the fact that the infrared-Raman and longitudinal-transverse symmetries are preserved in experiments on mixed compounds. This conservation of symmetry is very important for the experimentalists since they use it to follow the evolution of the mode frequencies with concentration. We have also explicitly shown, however (Figs. 11 and 12), that these symmetries are only approximate. They probably come from the fact that the modes that mix more strongly come from a given band and hence possess the same symmetry (longitudinal or transverse to the chain direction for example). While the preservation of the above symmetries in the mixed crystals has been recognized for a long time by experimentalists, our calculation is the first to our knowledge to exhibit this phenomenon for a linear-chain compound. It is interesting to speculate on what additional disorder must be introduce to break these symmetries. Some obvious suggestions come to mind.

(3) We have confirmed that for the model of Fig. 2(b), Raman lines are asymmetrical (Fig. 13), as in the real system, and that correlations reduce the asymmetry. We have also shown that contrary to the strictly one-dimensional chain and to what is more generally assumed,[36–40] the asymmetry cannot always be used to infer the curvature of the bands of the parent pure compounds. In the usual models,[36–40] there is no weight in the regions where the pure compounds have no eigenfrequencies. This assumption is fully justified when the Saxon-Hutner-Luttinger theorem[5] applies. In our model, the Raman band of interest is flat in the pure compound and nevertheless quite asymmetrical in the mixed compound.

(4) Within the polarizability model used here,[28–30] matrix-element disorder (polarizability disorder) can be as important as mass disorder (Fig. 4) in the determination of the Raman spectrum of the strictly one-dimensional chain. In the more realistic model of Fig. 2(b), however, polarizability disorder does not modify the spectra dramatically, but this is, in a sense, because contrary to the strictly one-dimensional chain, there are already very strong intensity Raman active lines even without polarizability disorder.

The following results apply qualitatively to both the strictly one-dimensional chain[4,8,9] and to the model of Fig. 2(b).

(5) In the cases where the calculated spectra have relatively narrow bandwidths, it is because the frequency range between the optic modes of the parent compounds is relatively narrow. In other words, it is a whole band, or large fraction of a whole band, which is excited in the disordered compounds. When one can identify a single "mode" in the spectrum of the disordered chain, it is in fact a very large number of modes which are excited, but the individual contributions are not resolved because of the relative value of the damping ϵ (anharmonicity). Note then that it is, in general, not necessary to invoke a change in anharmonicity to explain the broadening of the overall spectrum in the disordered compounds. In fact, in the one-band case we have studied (see below), quantitative agreement with the observed broadening at intermediate compositions can be obtained with a value of ϵ which does not change with composition.

(6a) Much emphasis has been put[3,4] in the past on the distinction between one-mode and two-mode behavior, or more appropriately, one-band and two-band behavior. One-band or multiband behavior can be observed in both the strictly one-dimensional chain and in the more elaborate model of Fig. 2(b) (Figs. 6 and 7). In the latter case, simple one-band behavior was observed (Fig. 7) for eigenmodes which are qualitatively similar to modes of the strictly one-dimensional model in the sense that they do not involve large relative displacements within the chalcogen cages. There are several points concerning one-band and two-band behavior which clearly stand out from the one-dimensional chain results. First, the distinction between one-band and two-band behavior is qualitative only with no sharp distinction between both types of behaviors. What happens in all cases, is that many modes are activated in the frequency interval between the optic modes of the parent compounds. The individual modes may or may not be resolved depending on anharmonicities. The "center of gravity" of the activated mode shifts progressively form the frequency of one compound to that of the other: sometimes the band of activated modes shifts in a block, sometimes in two separate blocks, in general in many blocks, and when the concentration is varied continuously, the concentration at which a change from one-band to two-band behavior occurs, when it does,

is not sharply defined. The discussions[4] on one-band behavior "with structure" and two-band behavior "with structure" are symptomatic of the purely qualitative difference between one- and two-band behavior. Second, while one- and two-band behavior may be correlated with the localization length of the modes, it is clearly not related to the distinction between localized and delocalized states: Indeed, in one dimension states are localized with probability one.[44]

(6b) The above considerations suggest that the fixed-point theory of Ref. 7, for example, should not be interpreted as indicating that the distinction between one-band and two-band behavior is of the same type as the distinction between two "phases" or that a change from one- to two-band behavior is like a phase transition. Another class of models which may be misleading is the isodisplacement theory.[4] While second-neighbor interactions are necessary in the latter approach to produce one-band behavior, we see that in the linear chain, one-band behavior can occur without such interactions. Second-neighbor interactions sometimes favor one-band behavior, sometimes they do not.[9] Isodisplacement models also suggest the existence of delocalized modes, but the linear-chain model clearly demonstrates that one-band behavior can be obtained with localized states. Isodisplacement models should be considered as a fitting procedure where some of the fitting parameters have a physical significance which is unclear.

Extensions of the present work could include a study of the influence of force-constant disorder on one-band behavior, and a more thorough investigation of the factors influencing the asymmetry of the Raman lines when the Saxon-Hutner-Luttinger theorem does not apply. Finally, note that our method of calculation is a generalization of the negative eigenvalue theorem[8,31,32] which allows an efficient computation of projected densities of states without explicit evaluation of all the eigenvectors and eigenvalues. Raman and infrared spectra are simply obtained from the same point of view by projection on different vectors.

ACKNOWLEDGMENTS

We are especially indebted to Robert Provencher for numerous illuminating discussions and for access to his experimental data. We should also like to thank S. Jandl and A. Caillé for numerous useful discussions and references. We have benefited from a critical reading of our manuscript by S. Jandl. Computing time was provided by the Centre de calcul de l'Université de Sherbrooke. J.M.L.C. was supported in part for international collaboration in research by the NATO Scientific Affairs Division (research grant No. 013.82) and in part by a France-Québec Exchange Program. A.-M.S. Tremblay would like to acknowledge the support of the Natural Science and Engineering Research Council of Canada.

[1]J. M. Ziman, *Models of Disorder* (Cambridge University Press, Cambridge, 1979).

[2]R. Shuker and R. W. Gammon, Phys. Rev. Lett. **25**, 222 (1970).

[3]F. I. Chang and S. S. Mitra, Adv. Phys. **20**, 359 (1971).

[4]A. S. Barker and A. J. Sievers, Rev. Mod. Phys. **47**, S1 (1975).

[5]D. S. Saxon and R. A. Hutner, Philips Res. Rep. **4**, 81 (1949), conjectured the result which was proven by J. M. Luttinger, Philips Res. Rep. **6**, 303 (1951). The generalization of interest for the present paper was given by J. Hori, Prog. Theor. Phys. (Osaka) **32**, 371 (1964); **32**, 471 (1964); and J. Hori and H. Matsuda, *ibid.* **32**, 183 (1964). See also, J. Hori, *Spectral Properties of Disordered Chains and Lattices* (Pergamon, Oxford, 1968); Proc. Phys. Soc. (London) **92**, 977 (1967). A summary of the various papers on this subject may be found in P. Erdös and R. C. Herndon, Adv. Phys. **31**, 65 (1982).

[6]P. N. Sen and W. M. Hartmann, Phys. Rev. B **9**, 367 (1974).

[7]D. Schmeltzer and R. Beserman, Phys. Rev. Lett. **47**, 860 (1981).

[8]M. A. Lemieux, P. Breton, and A.-M. S. Tremblay, J. Phys. (Paris) Lett. **46**, L1 (1985).

[9]A.-M. S. Tremblay and P. Breton, J. App. Phys. **55**, 2389 (1984).

[10]S. Furnseth, L. Brattas, and A. Kjekshus, Acta Chem. Scand. Ser. **A29**, 623 (1975).

[11]W. Krönert and K. Plieth, Z. Anorg. Allg. Chem. **336**, 207 (1965).

[12]S. Jandl, C. Deville Cavellin, and J. Y. Harbec, Solid State Commun. **31**, 351 (1979).

[13]S. Jandl, M. Banville, and J. Y. Harbec, Phys. Rev. B **22**, 5697 (1980).

[14]A. Zwick and M. A. Renucci, Phys. Status Solidi B **96**, 757 (1979).

[15]A. Grisel, F. Lévy, and T. J. Wieting, Physica **99B**, 365 (1980).

[16]C. Deville Cavellin and S. Jandl, Solid State Commun. **33**, 813 (1980).

[17]S. Jandl and J. Deslandes, Can. J. Phys. **59**, 936 (1981).

[18]S. Jandl and R. Provencher, J. Phys. C **14**, L461 (1981).

[19]R. Provencher, S. Jandl, and C. Carlone, Phys. Rev. B **26**, 7049 (1982).

[20]A. Zwick, G. Landa, M. A. Renucci, R. Carles, and A. Kjekshus, Phys. Rev. B **26**, 5694 (1982).

[21]A. Zwick, G. Landa, R. Carles, M. A. Renucci, and A. Kjekshus, Solid State Commun. **45**, 889 (1983).

[22]J. Deslandes and S. Jandl, Phys. Rev. B **29**, 2088 (1984).

[23]J. Deslandes and S. Jandl, Phys. Rev. B **30**, 6019 (1984).

[24]C. Sourisseau and Y. Mathey, Chem. Phys. **63**, 143 (1981); T. J. Wieting, A. Grisel, and F. Lévy, Physica **105B**, 366 (1981).

[25]M. Poirier and P.-E. Séguin, Solid State Commun. **54**, 375 (1985).

[26]D. A. Long, *Raman Spectroscopy* (McGraw-Hill, New York, 1977).

[27]M. Born and K. Huang, *Dynamical Theory of Crystal Lattices* (Oxford, Oxford, 1954).

[28]R. Alben, J. E. Smith, Jr., M. H. Brodsky, and D. Weaire, Phys. Rev. Lett. **30**, 1141 (1973).

[29]R. Alben, D. Weaire, J. E. Smith, Jr., and M. H. Brodsky, Phys. Rev. B **11**, 2271 (1975).

[30]Sammy Go, Heinz Bilz, and Manuel Cardona, Phys. Rev. Lett. **34**, 580 (1975).
[31]P. Dean, Rev. Mod. Phys. **44**, 127 (1972).
[32]M. A. Lemieux and A.-M. S. Tremblay (unpublished).
[33]L. Brattäs and A. Kjekshus, Acta Chem. Scand. **26**, 3441 (1972).
[34]R. Provencher, Master's thesis, Université de Sherbrooke, 1982 (unpublished).
[35]P. N. Keating, Phys. Rev. **145**, 637 (1966).
[36]B. Jusserand and J. Sapriel, Phys. Rev. B **24**, 7194 (1981).
[37]T. N. Krabach, N. Wada, M. V. Klein, K. C. Cadien, and J. E. Green, Solid State Commun. **45**, 895 (1983).
[38]H. Richter, Z. P. Wang, and L. Ley, Solid State Commun. **39**, 625 (1981).
[39]K. K. Tiong, P. M. Amirtharaj, F. H. Pollak, and D. E. Aspnes, Appl. Phys. Lett. **S44**, 122 (1984).
[40]P. Parayanthal and F. H. Pollak, Phys. Rev. Lett. **52**, 1822 (1984).
[41]M. A. Lemieux and A.-M. S. Tremblay (unpublished).
[42]R. Provencher (private communication).
[43]See, for example, J. Canisius and J. L. van Hemmen, J. Phys. C **18**, 4873 (1985), for a study of the mobility edge in the case of binary mass disorder in two and three dimensions; and S. Y. Wu and Z. Zheng, Phys. Rev. B **24**, 4787 (1981), for the one-dimensional case.
[44]We have seen, however, that one of the zone-edge modes is delocalized in the mixed crystals we have considered.